

Zonal flow formation in the stellarator TJ-K

B. Schmid¹, M. Ramisch¹, U. Stroth^{2,3}

¹ IGVP, Universität Stuttgart, 70569 Stuttgart, Germany

² Max-Planck-Institut für Plasmaphysik, 85748 Garching, Germany

³ Physik-Department E28, Technische Universität München, 85747 Garching, Germany

Introduction Zonal flows are an integral part of various types of turbulence. In fusion science, they are of particular interest because they are supposed to be linked to the H-mode transition. Because of their symmetry these turbulent structures do not contribute to turbulent cross-field transport, and can suppress radial transport by shearing off drift-wave eddies. Like in a self-organization process, the zonal flow is generated by the ambient turbulence itself and is therefore often referred to as secondary instability. Drift-wave eddies are tilted and drive the shear flow, which leads to a self-amplification of the zonal flow. The tilt can be measured by the so-called Reynolds stress. For zonal-flow growth, only the flux-surface averaged Reynolds stress is normally considered. Nevertheless, the Reynolds stress is a local quantity and its distribution is important to understand the Reynolds-stress drive. The zonal flow is a result of nonlinear interaction of drift waves. For this reason, bispectral analyses are the preferred method to investigate this three-wave coupling.

Stellarator TJ-K The experiments were carried out in the low-temperature plasmas of the stellarator TJ-K. It was shown that the turbulence is drift-wave dominated and normalised quantities are similar to fusion edge plasmas [1]. The whole confinement region is thereby accessible to Langmuir probes. Therefore, ion-saturation current ($\tilde{I}_{i,sat}$) and floating potential ($\tilde{\phi}_f$) can be acquired with high spatial and temporal resolution. They can be related to density ($\tilde{I}_{i,sat} \propto \tilde{n}$) and plasma potential fluctuation ($\tilde{\phi}_f \propto \tilde{\phi}_{pl}$), because temperature fluctuations are small. Using two neighbouring probes the electric field

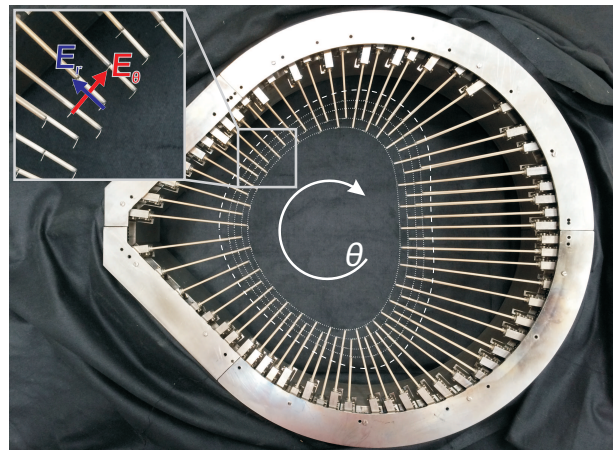


Figure 1: Poloidal Reynolds-stress array with Langmuir probes on four flux surfaces (dotted white lines) just inside the separatrix (dashed white line). The detail illustrates how the electric field components are measured.

is measured and the $E \times B$ -drift velocity is given by $v^{E \times B} \approx (\tilde{\phi}_{\text{fl},2} - \tilde{\phi}_{\text{fl},1}) / (B dx)$, where dx denotes the probe distance. Measuring both velocity components in the poloidal cross section, the Reynolds stress is then given as the product of fluctuations in radial \tilde{v}_r and poloidal \tilde{v}_θ velocity

$$R = \langle \tilde{v}_r \tilde{v}_\theta \rangle \approx \left\langle \frac{(\tilde{\phi}_{\text{fl},2} - \tilde{\phi}_{\text{fl},1})_r (\tilde{\phi}_{\text{fl},2} - \tilde{\phi}_{\text{fl},1})_\theta}{dr d\theta B^2} \right\rangle.$$

To study the driving mechanism the Reynolds stress has to be measured on different flux surfaces. Therefore, a poloidal probe array was used consisting of 128 Langmuir probes with 32 probes on each of four neighbouring flux surfaces (Figure 1). The probes are placed in the edge of the confined region where the density gradient is highest. For every measurement, 2^{20} data points were taken with a sampling rate of 1 MHz. The measurements were carried out in Helium discharges heated with microwaves at 2.45 GHz.

Poloidal Reynolds-stress distribution The Reynolds-stress array is designed for an outer port at TJ-K. There, the flux surfaces (white lines in Figure 1) have a triangular shape with an up-down symmetry. In Figure 2, the poloidal dependence of the fieldline-curvature components is shown. The normal curvature κ_n (b) becomes negative on the outboard side, whereas the geodesic curvature κ_g (c) has a sinusoidal form and changes sign at the midplane similar to tokamak geometry. With the probe configuration of the poloidal array the Reynolds stress R can be calculated at 32 positions on one flux surface. The temporal average over the full time traces is shown in Figure 2 (a). Non-zero values are mainly present on the outboard side in regions of negative ('bad') normal curvature κ_n . A pronounced maximum is visible above the midplane ($\theta \approx 0.3\pi$) indicated by the grey area. In this region the normal curvature is still negative whereas the geodesic curvature is positive. A similar behaviour has been found for the local cross-field transport $\Gamma = \langle \tilde{v}_r \tilde{n} \rangle$ [2]. Since the Reynolds stress can be seen as the radial transport of poloidal momentum a comparable influence of the curvature terms is supposed.

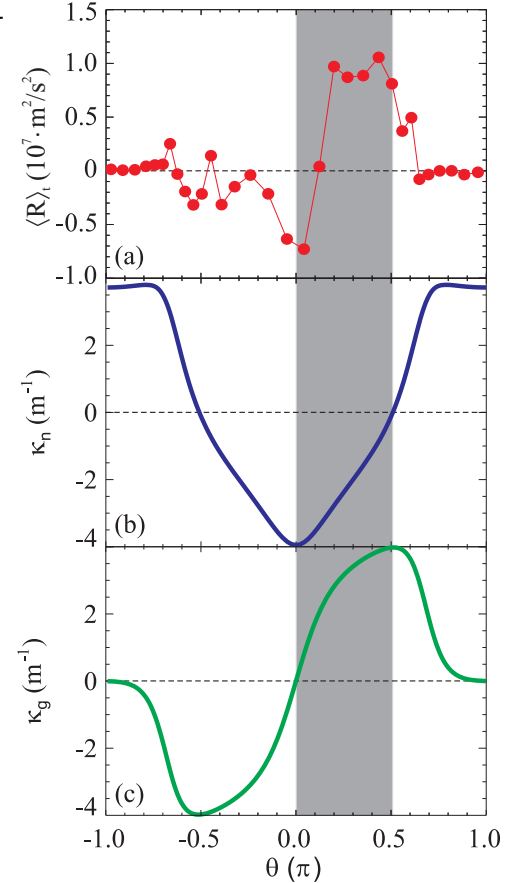


Figure 2: Poloidal distribution of the time averaged Reynolds stress (a), the normal curvature (b) and the geodesic curvature (c).

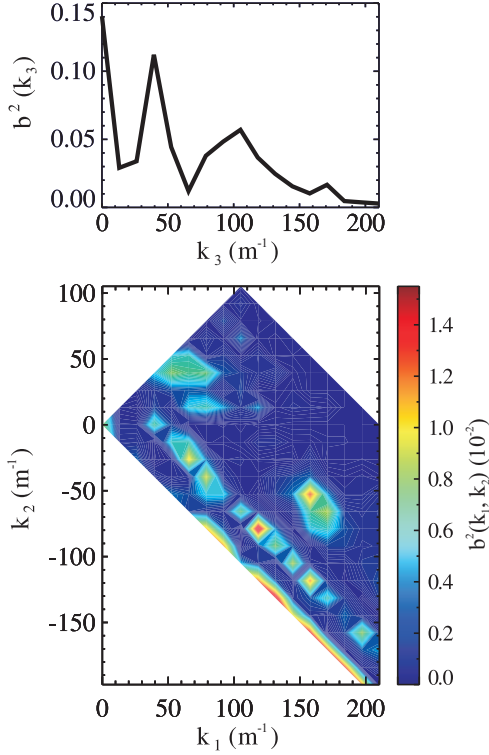


Figure 3: Quadratic crossbicoherence spectrum in wavenumber space (lower plot) and the integrated spectrum (upper plot) showing the coupling to the $k_3 = 0$ mode.

Drift wave - zonal flow interaction The array can also be used in a mixed mode, where on two of the four flux surfaces ion-saturation current is measured. In this operation mode the Reynolds stress cannot be determined anymore, but information about density and potential fluctuations is accessible simultaneously. Because the zonal flow occurs in consequence of three-wave coupling of drift waves, the interaction should be present in a crossbispectrum $B_{x,y,z}(k_1, k_2)$ [3]. For a constant biphasic relation between the constituents x, y and z the cross-bicoherence takes non-zero values. The quadratic crossbicoherence may be written with the Fourier transformations \hat{x} , \hat{y} , \hat{z} as

$$b_{x,y,z}^2(k_1, k_2) = \lim_{L \rightarrow \infty} \frac{|\langle \hat{x}_L(k_1, t) \hat{y}_L(k_2, t) \hat{z}_L^*(k_1 + k_2, t) \rangle|^2}{\langle |\hat{x}_L(k_1, t)|^2 \rangle \langle |\hat{z}_L(k_1 + k_2, t)|^2 \rangle},$$

where the resonance condition $k_3 = k_1 + k_2$ is satisfied. To investigate the coupling analogue to the density fluctuation activity transfer [4] spatial density ($x(\theta, t)$, $y(\theta, t)$) and potential ($z(\theta, t)$) data of a flux surface is used. Through cross-coupling of \tilde{n} to $\tilde{\phi}$ also drift wave - zonal flow interaction is included. As the zonal flow is an intermittent event and its duration covers only less than 7% of the full time trace, the fraction of its three-wave coupling in the overall spectrum is small. Applying conditional averaging technique, nearly 373k realizations around the zonal-flow occurrence are extracted and used for the ensemble average $\langle . \rangle$.

The contour plot in Figure 3 shows the non-redundant part of the crossbicoherence spectrum. Above this the integrated quadratic crossbicoherence

$$b_{x,y,z}^2(k_3) = \sum_{k_1, k_2} b_{x,y,z}^2(k_1, k_2) \delta_{k_1+k_2, k_3}$$

can be seen, which represents the overall coupling to the k_3 potential mode. It is the sum over all components on parallels to the $k_2 = -k_1$ line. The integrated bicoherence $b^2(k_3)$ shows a maximum for the $k_3 = 0$ potential mode, which is the zonal flow. In the bicoherence $b^2(k_1, k_2)$, the contribution of many different density modes is visible on the corresponding diagonal. It shows that mostly higher density mode numbers couple to the zonal flow. This is a sign for the non-local inverse cascade, where the zonal flow is driven by small scale drift-wave structures [5, 6].

Conclusion Detailed studies using a multi-Langmuir-probe array have been carried out on the stellarator TJ-K to investigate the zonal-flow drive. Thereby, the poloidal dependence of the Reynolds stress was resolved and a strong poloidal asymmetry was found. A maximum is present where the normal curvature is negative and the geodesic curvature is positive, which is similar to the behaviour of local cross-field transport. To study the process of three-wave coupling between the drift waves and the zonal flow, the quadratic crossbicoherence spectrum was calculated in wavenumber space. There, a broad coupling of small-scale drift waves to the zonal flow is found. The result is consistent with the non-local inverse cascade assumed for drift wave - zonal flow interaction.

References

- [1] U. Stroth et al., Phys. Plasmas **11**, 2558 (2004).
- [2] G. Birkenmeier et al., Phys. Rev. Lett. **107**, 025001 (2011).
- [3] Y. K. Kim et al., Phys. Fluids **8**, 1452 (1978).
- [4] S. J. Camargo et al., Phys. Plasmas **2**, 48 (1995).
- [5] P. H. Diamond et al., Plasma Phys. Controlled Fusion **47**, R35 (2005).
- [6] P. Manz et al., Phys. Rev. Lett. **103**, 165004 (2009).